Enhanced attosecond pulse generation in the vacuum ultraviolet using a two-colour driving field for high harmonic generation

P. Matía-Hernando[a], T. Witting[a*], D. J. Walke[a], J. P. Marangos[a] and J. W. G. Tisch[a†]

[a]Blackett Laboratory, Imperial College London, London SW7 2AZ, UK

ARTICLE HISTORY
Compiled July 8, 2017

ABSTRACT
High-harmonic radiation in the extreme ultraviolet and soft X-ray spectral regions can be used to generate attosecond pulses and to obtain structural and dynamic information in small atoms and molecules. However, these sources typically suffer from a limited photon flux, and the spectral filtering required for the isolation of attosecond pulses can lead to the appearance of satellites in the time domain, limiting their temporal resolution. The use of multi-colour driving fields has been proven to enhance the harmonic yield and provide additional control, using the relative delays between the different spectral components for waveform shaping. We describe here a two-colour high-harmonic source that combines few-cycle near-infrared pulse with a multi-cycle second harmonic component, with both relative phase and carrier-envelope phase stabilization. We observe strong modulations in the harmonic flux, and present simulations and experimental results supporting the suppresion of satellites in sub-femtosecond pulses at 20 eV compared to the single colour field case, an important requirement for attosecond pump-probe measurements.

KEYWORDS
nonlinear and ultrafast optics; attosecond science; multi-colour fields; coherent control; high-order harmonic generation

1. Introduction

High-harmonic generation (HHG) is a nonlinear interaction between matter and an intense laser field that results in the coherent emission of highly energetic photons. It was first observed in gases in the late 1980s (*1*, *2*), and since 2000 it has proven to be an invaluable tool of attosecond science due to its characteristic temporal confinement. The process of HHG can be used to generate pulses below 200 attoseconds of duration in the extreme ultraviolet and soft X-ray spectral regions (*3*), which can be used in pump-probe experiments. Furthermore, the high degree of coherence of the process can be applied to HHG spectroscopy, where we can perform structural measurements in small atoms and molecules as well as probe nuclear dynamics (*4*).

The conversion efficiency of high-harmonic generation is low, typically below 10^{-5} (*5*), due to the weak single-atom response and difficult phase-matching requirements

* Current address: Max Born Institute for Nonlinear Optics and Short Pulse Spectroscopy, Max-Born-Strasse 2a, 12489 Berlin, Germany

†Corresponding author. Email: john.tisch@imperial.ac.uk

for efficient macroscopic build-up (*6*). This leads to attosecond sources with a limited photon flux, on the nanojoule level, which currently poses a major experimental challenge for the application of these sources to the measurement of electron dynamics in molecules (*7*). For molecular pump-probe experiments, the availability of subfemtosecond vacuum-ultraviolet (VUV, 10-20 eV) pulses is especially valuable as the interaction cross-sections are often very high in this photon energy range, but drop rapidly as the photon energy increases above 25 eV. Few-cycle pulses have been used to generate isolated attosecond pulses via amplitude gating (*8*), which relies on spectral filtering of the harmonic cutoff to select only the photons that have originated from the most intense half-cycle of the driving field. For photon energies in the harmonic plateau, spectral filtering of several individual harmonics may be required (*9*), leading to a train of a small number of pulses or the appearance of satellites in the temporal profile of the pulse. This limits the temporal resolution achievable and reduces the power contained in the strongest pulse. Polarization gating (*10*) and double optical gating (*11*), both relying on the strong ellipticity dependence of HHG, have also been developed extensively, but at photon energies well below the harmonic cutoff they have been predicted to yield elliptically polarized attosecond pulses (*12*). In this paper we describe work focused on increasing the energy and contrast of attosecond pulses using a two-colour driving field, where a second harmonic component is added to a few-cycle pulse as additional temporal gating.

Due to its highly nonlinear character, HHG is very sensitive to the waveform of the driving pulse, and carefully engineered field profiles can be used to influence the process at the single-atom level, by enhancing ionisation at given times or steering the trajectory of electrons in the continuum. The addition of a weak second or third harmonic beam has been shown to increase the high-harmonic yield up to two orders of magnitude, as well as to extend the harmonic cutoff towards higher energies, with the instantaneous value of the combined electric field controlled by the relative phase between the two frequency components (*13–15*). The addition of non-commensurate fields has also been explored, often combining a near-infrared field with a longer wavelength component generated through optical parametric amplification (*16–18*), and obtained similarly promising effects on harmonic yield and cutoff. Orthogonally polarised multi-colour fields have also been used to control the relative contributions of different electron trajectories via the steering of the recolliding electron wave packet towards the parent ion (*19*, *20*). Related experiments have used an attosecond pulse train to initiate the high-harmonic generation process via single-photon ionization, selecting specific quantum trajectories via the relative delay between the fundamental driving field and the assisting harmonic beam (*21*, *22*). Furthermore, theoretical work has suggested that the optimized waveform to maximize the electron collision energy for a given frequency consists of a linear ramp with a dc component; this was subsequently implemented by combining a small number of below-threshold harmonics (*23*, *24*). Light transients, with a FWHM duration down to 380 attoseconds, have been generated by recombining four independently-compressed frequency components originating from an ultrabroadband frequency continuum (270-1130 nm) (*25*, *26*).

A crucial ingredient of all multi-colour HHG schemes is a fine control of time delays between the different components. In the case of long pulses, it can be introduced as a change in relative phase, but when few-cycle pulses are involved both the relative phase and the carrier-envelope phase (CEP) of the individual pulses require stability (*27*). We have developed a phase-stabilized two-colour high-harmonic source by combining a CEP-stabilized few-cycle near-infrared (NIR) beam with a longer second harmonic component, and studied the resulting harmonic spectra as a function of the delay

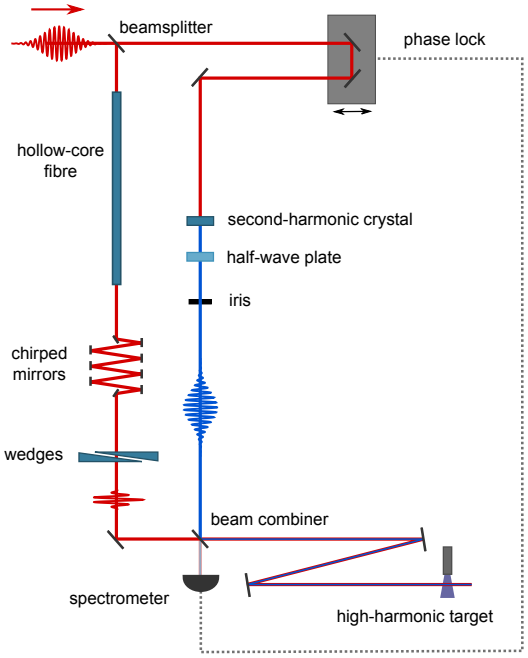


Figure 1. Experimental setup for two-colour high-harmonic generation.

between the two pulses. With the correct phase between the two fields we observe the generation of even order harmonics in the vacuum ultraviolet (VUV), which under our conditions is consistent with the generation of an attosecond pulse at 20 eV with significantly reduced satellite pulses compared to the NIR driving field only.

2. Experimental setup

The experimental setup is shown in figure 1. A chirped-pulse amplification laser system operating at a repetition rate of 1 kHz (Femtolaser GmbH, Femtopower HE) emits 30 fs pulses centered at a wavelength of 790 nm, with an energy up to 2.5 mJ per pulse. The output from this source was divided in two beams by a 50/50 beamsplitter, consisting of a broadband low-dispersion coating on a 1 mm fused silica substrate (FemtoOptics, OA237). The reflected beam was focused into a hollow-core fibre differentially pumped with neon gas, where the pulses were spectrally broadened via self-phase modulation and compressed to few-cycle duration with a set of chirped mirrors and a pair of fused silica wedges (*28*). The CEP of these few-cycle pulses was locked with a feedback system consisting of a pair of f-to-2f interferometers, with residual shot-to-shot fluctuations below 250 mrad (*29*). The beam transmitted by the beamsplitter was loosely focused into a thin BBO nonlinear crystal for type-I second-harmonic generation. A broadband half-wave plate was used to rotate the polarization of the second harmonic beam to match the fundamental.

Both arms were recombined with a fused silica substrate of 3 mm thickness, with a anti-reflection coating between 600 and 980 nm and high reflectivity coating centred around 400 nm, as well as low dispersion in both spectral regions (Layertec, 103510). The residual NIR beam used to generate the second harmonic beam was transmitted almost completely by the combiner and therefore did not contribute to the combined

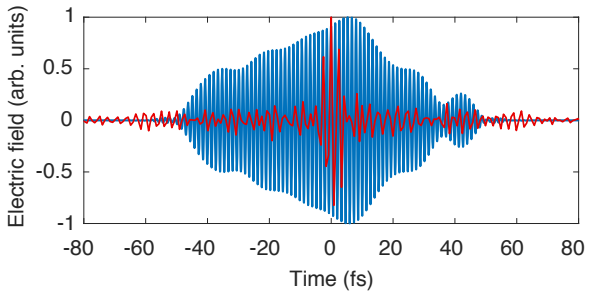


Figure 2. *(Red):* Electric field of the fundamental beam, characterised via SEA-F-SPIDER, corresponding to an intensity profile with a FWHM of 4.6 fs. *(Blue):* Electric field of the second harmonic beam, characterised via ARIES, corresponding to an intensity profile with a FWHM of 28 fs.

two-colour field. The spatial overlap of the two beams was optimized in the near field as well as in the far field with the aid of a reimaging system. After the combiner, the energy in the few-cycle NIR beam and the second harmonic beam was 450 μJ and 45 μJ respectively.

Temporal overlap between the two arms of the interferometer was controlled with a commercial spectrometer (HR4000CG-UV-NIR, Ocean Optics) that monitored the interference after the beam combiner between the residual NIR radiation reflected from the fundamental arm of the interferometer and that transmitted from the second harmonic arm. Due to the long optical path required to generate the few-cycle beam, the interferometer required active stabilisation, which was achieved with a piezo-controlled delay stage with sub-nanometer spatial resolution and a range of 38 μm (Physik Instrumente GmbH, P-753). After stabilisation, the residual fluctuations had a statistical shot-to-shot standard deviation below 200 mrad of the fundamental field.

The combined $\omega + 2\omega$ field was focused by a spherical mirror with a focal length of 75 cm, inside a vacuum chamber where two gas targets filled with neon and krypton gas can be used to generate high harmonic radiation in the XUV and VUV spectral regions, with each target optimised for generation at different wavelengths (*9*).

We have characterised the temporal profile of the fundamental component via spatially-resolved spectral shearing interferometry (SEA-F-SPIDER) (*30*), obtaining a full width at half maximum of 4.6 fs, limited by the thickness of the beam combiner substrate and the bandwidth and phase of its coating. The electric field is shown in red in figure 2. Furthermore, taking advantage of the existing high-harmonic setup we have characterised the waveform of the second harmonic field via attosecond-resolved interferometric electric-field sampling (ARIES) (*31*). This all-optical in situ characterisation technique can retrieve arbitrary optical waveforms using the linear cutoff energy shift induced by a weak test pulse in the high harmonic spectrum of an auxiliary strong field, as a function of the delay between the two fields. The full width at half maximum of the retrieved intensity envelope of the second harmonic field is 28 fs, and the electric field is shown in blue in figure 2.

3. Results

We have previously obtained harmonic spectra driven with a few-cycle NIR beam, shown in figure 3 and obtained with a flat-field imaging XUV spectrometer fitted with an microchannel plate and a CCD camera. After spectral filtering, the radiation generated around 90 eV was shown via attosecond streaking to support an isolated

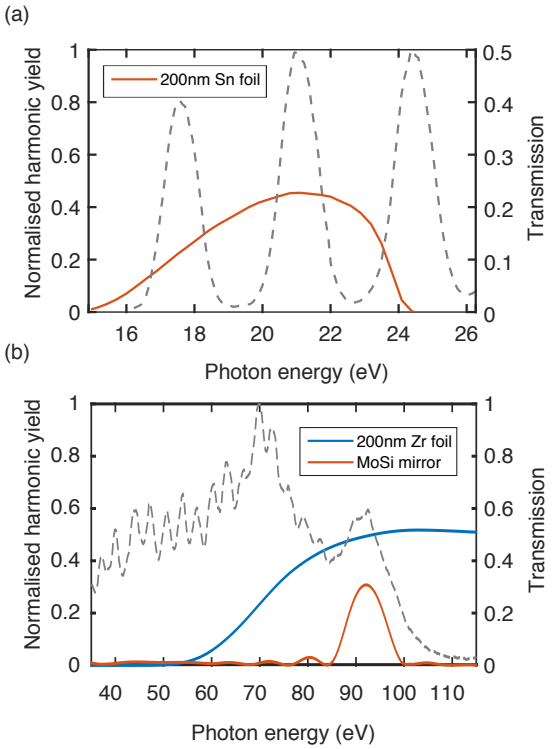


Figure 3. (a) HHG spectrum of krypton driven by a few-cycle NIR beam, together with the transmission curve of a 200 nm tin foil. (b) HHG spectrum of neon driven by a few-cycle NIR beam, together with the transmission curve of a 200 nm tin foil and the reflectivity of multilayer MoSi mirror designed for high reflectivity at the 90 eV cutoff.

attosecond pulse with a FWHM of the intensity profile of approximately 300 attoseconds (*9*). The VUV spectrum, filtered by a metallic foil centred at 20 eV, was also characterised and found to support a pulse with a sub-femtosecond FWHM and second moment, but in the shape of a train of attosecond pulses: two small satellites are present at ± 1.3 fs from the main peak, with an intensity around 0.4 of the main peak.

In this work, we have measured the high-harmonic spectra generated by the two-colour field as a function of the delay between the two fields. For these measurements, the ratio of intensity between the fields was $I_{2\omega}/I_{\omega} = 0.03$, obtained from the pulse energies and durations as well as beam spot measurements performed by reimaging the foci onto a CCD camera. The fields had parallel polarisation, and we verified that the second harmonic field was not strong enough to generate harmonics on its own. Figure 4 shows the results obtained in a neon gas jet, where the harmonic radiation was optimised to reach a cutoff around 90 eV. The vertical lineout shown on the left hand side shows oscillations in the cutoff at the frequency of the second harmonic beam. The horizontal lineouts, for two delays that differ by one half-cycle of the second harmonic beam, show for one particular delay an increase in harmonic yield in the spectral continuum together with a reduction of the cutoff to around 65 eV. This can be understood as arising from the second harmonic field increasing the total field at the time of ionisation (thus increasing the harmonic yield), but reducing the total field during the electron wavepacket acceleration phase (thus decreasing its energy upon recollision). Our increase in flux with respect to the fundamental-only HHG is not as pronounced as the improvements of up to two orders of magnitude previously reported (*15*), from which we conclude that our generation conditions were closer to saturation.

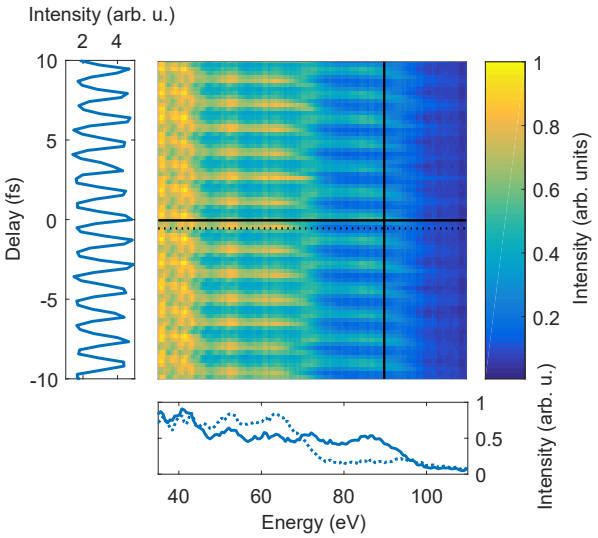


Figure 4. Spatially-integrated harmonic spectrum in neon driven by the two-colour field, as a function of the delay between the two fields. The vertical lineout shows a 2ω oscillation of the cutoff yield. The horizontal lineout shows the harmonic spectrum at two delays between the ω and 2ω fields separated by one half-cycle of the latter.

The corresponding result for the lower harmonic orders, generated in a krypton gas jet, is shown in figure 5. Even harmonic orders, typically absent from high harmonic spectra due to half-cycle symmetry, appear with intensities comparable to the neighbouring odd orders when this symmetry is disrupted. The yield of the even harmonics as a function of delay, marked by the vertical solid line in the main figure, is modulated at twice the frequency of the second harmonic field, as shown in the lineout on the left side of the figure, corresponding to the periodicity with which the combined field retains half-cycle symmetry. The modulation in the yield of the odd harmonics, shown with a dashed line, has a frequency of 2ω, and there is a phase shift between neighbouring harmonics as a result of the different excursion times of the returning electron wavepackets (*32*).

Let us now consider the potential of two-colour HHG for temporal shaping of attosecond pulses. As discussed before, attosecond streaking (*33*) and a FROG-CRAB retrieval method (*34*) have been used to characterise the VUV pulse that can be obtained by spectrally filtering the harmonic radiation around 20 eV with a 200 nm tin foil (*9*). Due to a transmission window that spans multiple harmonics, the resulting temporal intensity profile had a FWHM duration of 585±31 attoseconds, but with two satellites at a height of approximately 0.4 of the main peak, and spaced by one half cycle of the ω driving field from the main peak. This relatively large satellites are problematic for pump-probe experiments, where the VUV pulse triggers single-photon transitions with a probability that scales linearly with temporal intensity.

To study the effect of a two-colour driving field on attosecond VUV pulse generation, we have conducted numerical simulations solving the time-dependent Schrödinger equation (TDSE) for a model krypton atom with intensity averaging (*12*). The results of these simulations, shown in figure 6, demonstrate that the addition of a second harmonic field can considerably affect the temporal profile of the resulting VUV pulses, suppressing the satellite pulses compared to the fundamental-only case for small relative delays between the two pulses, with an optimum phase delay around 0.2π of the fundamental.

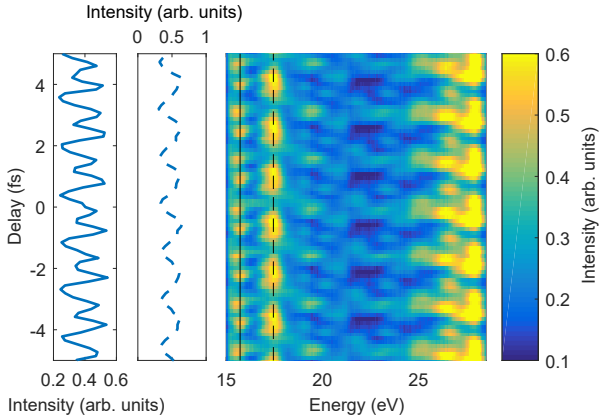


Figure 5. Spatially-integrated harmonic spectrum in krypton driven by the two-colour field, as a function of delay between the two fields. The leftmost vertical lineout shows 4ω oscillations of the yield of the even harmonics (solid line), while the second vertical lineout shows 2ω oscillations of the yield of the odd harmonics (dashed line).

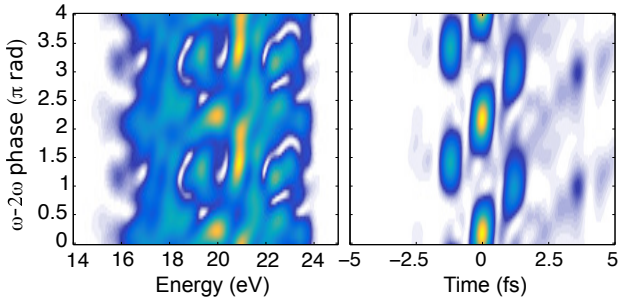


Figure 6. Scan of the phase between the phase-locked fundamental and second harmonic fields. *Left*: HHG spectrum obtained from SFA simulations with intensity averaging, after spectral filtering with a 200 nm tin foil. *Right*: Temporal intensity of the resulting VUV pulses. The two pulses are a 3.5 fs FWHM near-infrared centred at 750 nm, with a peak intensity of 4×10^{14} W/cm^2, and its second harmonic, obtained by numerical second-harmonic generation in a 100 μm BBO crystal ($\theta = 29.5°$), with central wavelength of 396 nm and a peak intensity of 0.04×10^{14} W/cm^2.

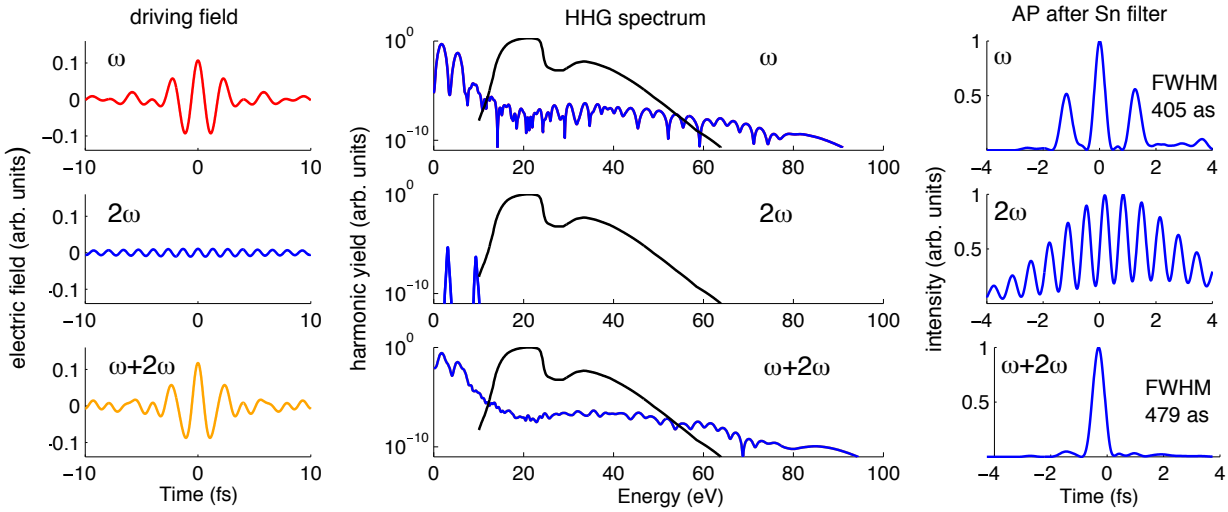


Figure 7. Comparison of simulated HHG with single-colour and two-colour driving pulses. *Left column*: Electric field of driving pulse. *Middle column*: HHG spectrum obtained from SFA simulations, on a logarithmic scale (blue line), together with the transmission window of a 200 nm tin foil (black line). *Right column*: VUV beam in the time domain after spectral filtering.

This prediction is shown in more detail in figure 7, where harmonic spectra were calculated for each of the components of the multicolour field as well as the coherent combination of the two fields at temporal overlap. The temporal profile of the resulting attosecond pulses, obtained in the VUV spectral range after applying the transmission window of a tin foil, shows that the addition of the second harmonic leads to a clear reduction of the satellites while maintaining sub-femtosecond duration of the main pulse. These predictions are consistent with our experimental results: figure 8 shows the spatially-resolved VUV spectrum generated in krypton obtained with the fundamental field only, as well as with the $\omega + 2\omega$ field with a relative phase delay optimised for satellite suppression. We have numerically applied the transmission curve corresponding to a 200 nm thick tin filter and obtained the Fourier transform of the resulting spectrum assuming a flat phase. We can see a decrease in the height of the satellite pulses to around 0.03 times the height of the main peak, optimised at the delay corresponding to strongest odd harmonics. A full attosecond streaking characterisation of the VUV pulses will be carried out in the near future.

4. Conclusions

We have demonstrated an actively stabilized two-colour field synthesizer setup for high-harmonic generation that coherently combines a 4.6 fs CEP-stable NIR beam and a 28 fs second-harmonic component. We have observed sub-cycle modulations in the harmonic yield at different orders as the delay between the two fields is scanned. We have obtained a two-fold increase in the harmonic flux, which would lead to attosecond pulses with a higher energy per pulse, an essential prerequisite for attosecond pump-probe measurements (*35*). Additionally, we have shown through experimental results and simulations the potential for a cleaner temporal profile with suppressed satellites for 20 eV sub-femtosecond pulses, which is another important requirement for many pump-probe experiments.

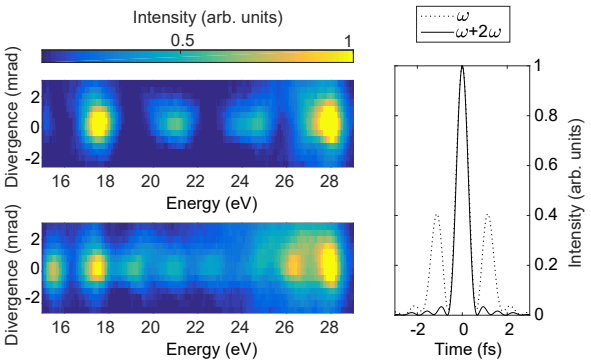


Figure 8. *Top left*: Spatially-resolved VUV spectrum generated in krypton when driven by fundamental field only. *Bottom left*: Spatially-resolved VUV spectrum generated in krypton when driven by the combined $\omega + 2\omega$ field at temporal overlap. *Right*: Intensity profile corresponding to the two spectra when filtered by a thin tin foil, assuming a flat phase.

Funding

This work was supported by the EPSRC Programme Grant No. EP/I032517/1; ERC ASTEX Project No. 290467; EC Marie Sklodowska-Curie ITN No. 317232; and EPSRC/DSTL MURI EP/N018680/1.

This paper is dedicated to the memory of Danny Segal, a valued friend and colleague, who we think would have appreciated this result.

References

(1) McPherson, A.; Gibson, G.; Jara, H.; Johann, U.; Luk, T.S.; McIntyre, I.A.; Boyer, K.; Rhodes, C.K. Studies of multiphoton production of vacuum-ultraviolet radiation in the rare gases, *Journal of the Optical Society of America B* **1987**, *4* (4), 595. http://www.opticsinfobase.org/abstract.cfm?uri=josab-4-4-595 https://www.osapublishing.org/abstract.cfm?URI=josab-4-4-595.

(2) Ferray, M.; L'Huillier, A.; Li, X.F.; Lompre, L.A.; Mainfray, G.; Manus, C. Multiple-harmonic conversion of 1064 nm radiation in rare gases, *Journal of Physics B: Atomic, Molecular and Optical Physics* **1988**, *21* (3), L31–L35. http://stacks.iop.org/0953-4075/21/i=3/a=001?key=crossref.96a70b41bd72507bfd3eb3689e112714.

(3) Drescher, M.; Hentschel, M.; Kienberger, R.; Tempea, G.; Spielmann, C.; Reider, G.A.; Corkum, P.B.; Krausz, F. X-ray pulses approaching the attosecond frontier., *Science (New York, N.Y.)* **2001**, *291* (5510), 1923–7. http://www.ncbi.nlm.nih.gov/pubmed/11239146.

(4) Lein, M. Molecular imaging using recolliding electrons, *Journal of Physics B: Atomic, Molecular and Optical Physics* **2007**, *40* (16), R135–R173. http://stacks.iop.org/0953-4075/40/i=16/a=R01?key=crossref.8141a9fd736394da72760a9362342556.

(5) Sansone, G.; Poletto, L.; Nisoli, M. High-energy attosecond light sources, *Nature Photonics* **2011**, *5* (11), 655–663. http://www.nature.com/doifinder/10.1038/nphoton.2011.167.

(6) Gaarde, M.B.; Tate, J.L.; Schafer, K.J. Macroscopic aspects of attosecond pulse generation, *Journal of Physics B: Atomic, Molecular and Optical Physics* **2008**, *41* (13), 132001. http://stacks.iop.org/0953-4075/41/i=13/a=132001?key=crossref.7b127d159c424b3a58da75b95c9fc9cf.

(7) Lépine, F.; Ivanov, M.Y.; Vrakking, M.J.J. Attosecond molecular dynamics: fact or fiction?, *Nature Photonics* **2014**, *8* (3), 195–204. http://www.nature.com/doifinder/10.1038/nphoton.2014.25.

(8) Goulielmakis, E.; Schultze, M.; Hofstetter, M.; Yakovlev, V.S.; Gagnon, J.; Uib-

eracker, M.; Aquila, A.L.; Gullikson, E.M.; Attwood, D.T.; Kienberger, R.; et al. Single-cycle nonlinear optics., *Science (New York, N.Y.)* **2008**, *320* (5883), 1614–7. http://www.ncbi.nlm.nih.gov/pubmed/18566281.

(9) Fabris, D.; Witting, T.; Okell, W.a.; Walke, D.J.; Matia-Hernando, P.; Henkel, J.; Barillot, T.R.; Lein, M.; Marangos, J.P.; Tisch, J.W.G. Synchronized pulses generated at 20 eV and 90 eV for attosecond pump-probe experiments, *Nature Photonics* **2015**, *9* (6), 383–387. http://www.nature.com/doifinder/10.1038/nphoton.2015.77.

(10) Sansone, G.; Benedetti, E.; Calegari, F.; Vozzi, C.; Avaldi, L.; Flammini, R.; Poletto, L.; Villoresi, P.; Altucci, C.; Velotta, R.; et al. Isolated single-cycle attosecond pulses., *Science (New York, N.Y.)* **2006**, *314* (5798), 443–6. http://www.ncbi.nlm.nih.gov/pubmed/17053142.

(11) Mashiko, H.; Gilbertson, S.; Li, C.; Khan, S.D.; Shakya, M.M.; Moon, E.; Chang, Z. Double Optical Gating of High-Order Harmonic Generation with Carrier-Envelope Phase Stabilized Lasers, *Physical Review Letters* **2008**, *100* (10), 103906. http://link.aps.org/doi/10.1103/PhysRevLett.100.103906.

(12) Henkel, J.; Witting, T.; Fabris, D.; Lein, M.; Knight, P.L.; Tisch, J.W.G.; Marangos, J.P. Prediction of attosecond light pulses in the VUV range in a high-order-harmonic-generation regime, *Physical Review A* **2013**, *87* (4), 043818. http://link.aps.org/doi/10.1103/PhysRevA.87.043818 https://link.aps.org/doi/10.1103/PhysRevA.87.043818.

(13) Watanabe, S.; Kondo, K.; Nabekawa, Y.; Sagisaka, A.; Kobayashi, Y. Two-Color Phase Control in Tunneling Ionization and Harmonic Generation by a Strong Laser Field and Its Third Harmonic, *Physical Review Letters* **1994**, *73* (20), 2692–2695. https://link.aps.org/doi/10.1103/PhysRevLett.73.2692.

(14) Kondo, K.; Kobayashi, Y.; Sagisaka, a.; Nabekawa, Y.; Watanabe, S. Tunneling ionization and harmonic generation in two-color fields, *Journal of the Optical Society of America B* **1996**, *13* (2), 424. https://www.osapublishing.org/abstract.cfm?URI=josab-13-2-424 http://www.opticsinfobase.org/abstract.cfm?URI=josab-13-2-424.

(15) Kim, I.; Kim, C.; Kim, H.; Lee, G.; Lee, Y.; Park, J.; Cho, D.; Nam, C. Highly Efficient High-Harmonic Generation in an Orthogonally Polarized Two-Color Laser Field, *Physical Review Letters* **2005**, *94* (24), 243901. http://link.aps.org/doi/10.1103/PhysRevLett.94.243901.

(16) Kim, B.; An, J.; Yu, Y.; Cheng, Y.; Xu, Z.; Kim, D.E. Optimization of multi-cycle two-color laser fields for the generation of an isolated attosecond pulse, *Optics Express* **2008**, *16* (14), 10331. https://www.osapublishing.org/oe/abstract.cfm?uri=oe-16-14-10331.

(17) Vozzi, C.; Calegari, F.; Frassetto, F.; Poletto, L.; Sansone, G.; Villoresi, P.; Nisoli, M.; De Silvestri, S.; Stagira, S. Coherent continuum generation above 100 eV driven by an ir parametric source in a two-color scheme, *Physical Review A - Atomic, Molecular, and Optical Physics* **2009**, *79* (3), 1–6.

(18) Siegel, T.; Torres, R.; Hoffmann, D.J.; Brugnera, L.; Procino, I.; Zaïr, A.; Underwood, J.G.; Springate, E.; Turcu, I.C.E.; Chipperfield, L.E.; et al. High harmonic emission from a superposition of multiple unrelated frequency fields, *Optics Express* **2010**, *18* (7), 6853. https://www.osapublishing.org/oe/abstract.cfm?uri=oe-18-7-6853.

(19) Brugnera, L.; Frank, F.; Hoffmann, D.J.; Torres, R.; Siegel, T.; Underwood, J.G.; Springate, E.; Froud, C.; Turcu, E.I.C.; Tisch, J.W.G.; et al. Enhancement of high harmonics generated by field steering of electrons in a two-color orthogonally polarized laser field., *Optics letters* **2010**, *35* (23), 3994–6. http://www.ncbi.nlm.nih.gov/pubmed/21124590 https://www.osapublishing.org/abstract.cfm?URI=ol-35-23-3994.

(20) Brugnera, L.; Hoffmann, D.J.; Siegel, T.; Frank, F.; Za??r, A.; Tisch, J.W.G.; Marangos, J.P. Trajectory selection in high harmonic generation by controlling the phase between orthogonal two-color fields, *Physical Review Letters* **2011**, *107* (15), 8–11.

(21) Schafer, K.J.; Gaarde, M.B.; Heinrich, A.; Biegert, J.; Keller, U. Strong Field Quantum Path Control Using Attosecond Pulse Trains, *Physical Review Letters* **2004**, *92* (2),

023003. https://link.aps.org/doi/10.1103/PhysRevLett.92.023003.
(22) Gaarde, M.; Schafer, K.J.; Heinrich, A.; Biegert, J.; Keller, U. Large enhancement of macroscopic yield in attosecond pulse train-assisted harmonic generation, *Physical Review A* **2005**, *72* (1), 013411. http://link.aps.org/doi/10.1103/PhysRevA.72.013411.
(23) Chipperfield, L.E.; Robinson, J.S.; Tisch, J.W.G.; Marangos, J.P. Ideal Waveform to Generate the Maximum Possible Electron Recollision Energy for Any Given Oscillation Period, *Physical Review Letters* **2009**, *102* (6), 063003. http://link.aps.org/doi/10.1103/PhysRevLett.102.063003 https://link.aps.org/doi/10.1103/PhysRevLett.102.063003.
(24) Haessler, S.; Balčiunas, T.; Fan, G.; Andriukaitis, G.; Pugžlys, A.; Baltuška, A.; Witting, T.; Squibb, R.; Zaïr, A.; Tisch, J.W.G.; et al. Optimization of Quantum Trajectories Driven by Strong-Field Waveforms, *Physical Review X* **2014**, *4* (2), 021028. http://link.aps.org/doi/10.1103/PhysRevX.4.021028 https://link.aps.org/doi/10.1103/PhysRevX.4.021028.
(25) Wirth, A.; Hassan, M.T.; Grguras, I.; Gagnon, J.; Moulet, A.; Luu, T.T.; Pabst, S.; Santra, R.; Alahmed, Z.A.; Azzeer, A.M.; et al. Synthesized Light Transients, *Science* **2011**, *334* (6053), 195–200. http://www.sciencemag.org/cgi/doi/10.1126/science.1210268.
(26) Hassan, M.T.; Luu, T.T.; Moulet, A.; Raskazovskaya, O.; Zhokhov, P.; Garg, M.; Karpowicz, N.; Zheltikov, A.M.; Pervak, V.; Krausz, F.; et al. Optical attosecond pulses and tracking the nonlinear response of bound electrons, *Nature* **2016**, *530* (7588), 66–70. http://www.nature.com/doifinder/10.1038/nature16528.
(27) Peng, D.; Pi, L.W.; Frolov, M.V.; Starace, A.F. Enhancing high-order-harmonic generation by time delays between two-color, few-cycle pulses, *Physical Review A* **2017**, *95* (3), 033413. https://link.aps.org/doi/10.1103/PhysRevA.95.033413.
(28) Robinson, J.S.; Haworth, C.; Teng, H.; Smith, R.; Marangos, J.P.; Tisch, J.W.G. The generation of intense, transform-limited laser pulses with tunable duration from 6 to 30 fs in a differentially pumped hollow fibre, *Applied Physics B* **2006**, *85* (4), 525–529. http://www.springerlink.com/index/10.1007/s00340-006-2390-z.
(29) Okell, W.A.; Witting, T.; Fabris, D.; Austin, D.; Bocoum, M.; Frank, F.; Ricci, A.; Jullien, A.; Walke, D.; Marangos, J.P.; et al. Carrier-envelope phase stability of hollow fibers used for high-energy few-cycle pulse generation, *Optics Letters* **2013**, *38* (19), 3918. http://www.opticsinfobase.org/abstract.cfm?URI=ol-38-19-3918 https://www.osapublishing.org/abstract.cfm?URI=ol-38-19-3918.
(30) Witting, T.; Frank, F.; Okell, W.A.; Arrell, C.A.; Marangos, J.P.; Tisch, J.W.G. Sub-4-fs laser pulse characterization by spatially resolved spectral shearing interferometry and attosecond streaking, *Journal of Physics B: Atomic, Molecular and Optical Physics* **2012**, *45* (7), 074014. http://stacks.iop.org/0953-4075/45/i=7/a=074014?key=crossref.93342f77093ffde7b75a11f16b0d5920.
(31) Wyatt, A.S.; Witting, T.; Schiavi, A.; Fabris, D.; Matia-Hernando, P.; Walmsley, I.A.; Marangos, J.P.; Tisch, J.W.G.; Walmsley, I.A. Attosecond sampling of arbitrary optical waveforms, *Optica* **2016**, *3* (3), 303. https://www.osapublishing.org/abstract.cfm?URI=optica-3-3-303.
(32) Dudovich, N.; Smirnova, O.; Levesque, J.; Mairesse, Y.; Ivanov, M.Y.; Villeneuve, D.M.; Corkum, P.B. Measuring and controlling the birth of attosecond XUV pulses, *Nature Physics* **2006**, *2* (11), 781–786. http://www.nature.com/doifinder/10.1038/nphys434.
(33) Itatani, J.; Quéré, F.; Yudin, G.; Ivanov, M.; Krausz, F.; Corkum, P.B. Attosecond Streak Camera, *Physical Review Letters* **2002**, *88* (17), 173903. http://link.aps.org/doi/10.1103/PhysRevLett.88.173903.
(34) Mairesse, Y.; Quéré, F. Frequency-resolved optical gating for complete reconstruction of attosecond bursts, *Physical Review A* **2005**, *71* (1), 011401. http://link.aps.org/doi/10.1103/PhysRevA.71.011401.
(35) Barillot, T.; Matia-Hernando, P.; Greening, D.; Walke, D.; Witting, T.; Frasinski, L.; Marangos, J.; Tisch, J. Towards XUV pump-probe experiments in

the femtosecond to sub-femtosecond regime: New measurement of the helium two-photon ionization cross-section, *Chemical Physics Letters* **2017**. http://linkinghub.elsevier.com/retrieve/pii/S0009261417304645.